Computational study of the electrochemical reduction of W(CO)4(2,2'-dipyridylamine)

(Article begins on next page)

14 January 2025

Laura Rotundo, Claudio Garino, Roberto Gobetto, Carlo Nervi.

Computational Study of the Electrochemical Reduction of W(CO)4(2,2'-dipyridylamine)

Laura Rotundo, Claudio Garino, Roberto Gobetto and Carlo Nervi*

Department of Chemistry and NIS (Centre of Excellence), University of Torino, Via P. Giuria 7, 10125, Torino, Italy, and Consorzio Interuniversitario Reattività Chimica e Catalisi (CIRCC), Bari.

Abstract

Quantum mechanical calculations on W(CO)$_4$(4,6-diphenyl-2,2'-bipyridine) (**1**) and on W(CO)$_4$(2,2'-dipyridylamine) (**2**) were performed with the aim to shed light on the nature of the electrochemical behaviour previously observed under Ar. DFT confirmed the stability of **1** after 1e reduction, showing agreement between IR-SEC (spectroelectrochemical) data and computed IR frequencies. It has been found that the nature of the electrochemical irreversible behaviour of **2** after 1e reduction is due to a geometry rearrangement in which a single pyridine ring is rotated. In long time scale of the IR-SEC a proton loss accounts for the observed IR spectra. Under CO$_2$ a mechanism of conversion to CO and carbonate ions are herein proposed, and the corresponding transition states individuated.

Introduction

Nowadays, there is the need of a radical breakthrough in energy supply technologies to cope with the depletion of fossil energy resources and to reduce global warming [1-5]. Several sustainable approaches have been pursued during last decades, and sunlight conversion plays the main role. One of the most interesting strategies is mimicking the natural photosynthesis process with the aim of converting carbon dioxide and water into chemical fuels and oxygen by using sunlight, thus adopting the carbon-cycle as energy vector for solar energy conversion. Potentially, any CO_2 reduction product precursor to fuels, like methanol, methane, CO, formic acid, etc., could be used in already known technologies, spanning from thermal engines to fuel cells. However, direct artificial photosynthesis of organic molecules is still far away from providing large-scale real-world solutions. Therefore, solar energy production by the well-established photovoltaic technology has been proposed to be employed in the electrochemical conversion of chemical feedstocks (like CO_2) in fuels by solar energy [2].

The electrochemical reduction of CO_2 to fuels and/or fuel precursors still requires low-cost, efficient and selective catalysts for a sustainable energy economy. In this context, homogeneous electrocatalysis is a suitable method to achieve the goal [6-8]. We recently explored the electrocatalytic properties of group 7 metals toward CO_2 reduction [9-11]. Much fewer systems based on lower-cost group 6 metals are known [12-17], and the understanding of their CO_2 reduction mechanism is still very limited. $M(CO)_4(diimine)$ complexes (M=Mo, W) usually undergo a first reversible 1e reduction followed by a second 1e chemically irreversible reduction, after which CO loss is observed. The resulting pentacoordinated species is supposed to be the active redox catalyst in CO_2 reduction. These observations have been recently reported by us also for the complex $W(CO)_4(4,6-diphenyl-2,2'-bipyridine)$ (**1**) [13]. On the other hand, we show that the analogue complex $W(CO)_4(dpa)$ (dpa=2,2'-dipyridylamine) (**2**) undergoes an unusual electrochemical behaviour, namely a single 1e irreversible reduction at rather negative potentials without CO loss. In this case a sustained catalytic activity has been observed under CO_2 atmosphere with a fivefold increase of the TON values for the conversion of CO_2 into CO. We thought that the dpa ligand could play a non-innocent role in the electrochemical reduction of CO_2 by $W(CO)_4(dpa)$. Indeed bpy and dpa only apparently are similar, providing completely different features to the complexes that they form [18]. The aim of this paper is to shed light by computational methods on the mechanism observed during the electrochemical reduction of **2**.

Experimental

Gaussian 09 Rev. D.01 was employed for all calculations [19]. Geometry optimizations were performed with the B3LYP functional including the conductor-like polarizable continuum model method (CPCM) [20] with acetonitrile as solvent. The LanL2DZ [21] basis sets were used for W, and 6–31G(d,p) for the other atoms. Unrestricted open-shell calculations were performed on the radical anions. The nature of all optimized structures was verified by using harmonic vibrational frequency calculations. No imaginary frequencies were found, thus indicating we had located the minima on the potential-energy surfaces. To compensate the neglecting of anharmonicity effects of the theoretical calculations, scale factor of 0.968 was applied to the computed quantum chemical harmonic vibrational frequencies [22]. In the manuscript we thoroughly reported the Gibbs free energies (ΔG).

Results and Discussion

Calculations on $W(CO)_4(4,6-diphenyl-2,2'-bipyridine)$ (**1**) and on its corresponding radical anion **1**$^-$ show that the optimized structures have almost the same geometry, in agreement with the reversibility of the first 1e reduction process observed during CV. Furthermore, the computed and experimental IR frequencies reasonably agree (Table 1) and the M-CO bonds lengths of **1** and **1**$^-$ are essentially equivalent.

Table 1. Experimental [13] and computed IR frequencies for the complexes under study.

Compound	Experimental IR-SEC (cm^{-1})	Computed IR (cm^{-1})	N–H (Å)
1	2006, 1885, 1826	2006, 1883, 1873, 1830	
1$^-$	1985, 1854, 1796	1989, 1854, 1846, 1802	
2	2010, 1885, 1865, 1818	2010, 1874, 1872, 1824	1.012
2$^-$		1924, 1838, 1825, 1788	1.011
3$^-$		1916, 1809, 1800, 1754	1.023
4$^-$		1917, 1810, 1796, 1773	1.022
5$^-$		2009, 1888, 1879, 1795	2.675^a
6$^-$	1996, 1868, 1843, 1795	1997, 1855, 1853, 1805	
7$^-$		1998, 1855, 1852, 1800	

^{a} The W-H bond length in the hydride **5$^-$** is 1.770 Å.

Geometry optimization of W(CO)$_4$(dpa) (**2**) shows that dpa coordinates W with py rings bent by 28.6° with respect to the plane that include W and the two equatorial COs. These W-CO bonds are shorter (1.973 Å) in comparison with the two axial COs (~2.046 Å). Concurrently, the two py rings of dpa are tilted by 43.4° one respect the other (Figure 1). This seems to suggest a low electron delocalization over the dpa ligand. Single crystal structure determinations show that for all the three complexes M(CO)$_4$(dpa) (M=Cr, Mo, W) the equatorial M-CO bonds are shorter than axial ones, [23] albeit in the solid state the crystal packing alter bond lengths and IR stretching frequencies. Interestingly, in the solid state intermolecular N-H⋯O=C hydrogen bonding is present that may alter the M-CO bond lengths.
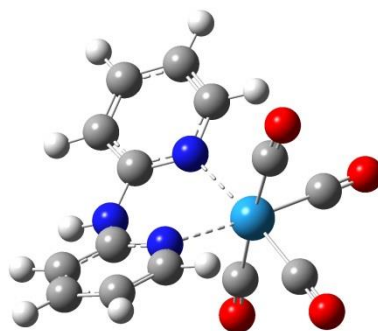
Fig. 1. Optimized geometry of **2**.

On the other hand, previous calculations of the radical anion show that electron spin density is equally distributed on the ligand, increasing the bending of dpa respect the equatorial plane from 28.6° to 31.3° and decreasing the tilting of the two py rings from 43.4° to 20.4°, with also a concomitant slightly strengthening of the W-CO bonds [13]. While these observations agree with the fact that no CO evolution is detected during the exhaustive electrolysis, they do not account for the chemical irreversible processes following the reduction of **2**. Furthermore, the DFT calculated IR stretching frequencies ν_{CO} of **2$^-$** (1924, 1838, 1825 and 1788 cm^{-1}) do not fit at all with the values observed in IR-SEC experiments (1996, 1868, 1843 and 1795 cm^{-1}) after 1e exhaustive electrolysis of **2** (Table 1). Several hypothesis ranging from Hofman degradation, [24] metal hydrides formation, [10, 11] and hydrogen abstraction from acetonitrile [10, 11, 25, 26] could be formulated if rather negative potentials are applied.

Intrigued by the structural modification displayed by the radical anion **2$^-$**, we decided to start from the DFT optimized structure of **2$^-$** and to search for a transition state, **TS2$^-$**, in which one of the two py rings could rotate and point away from the metal. Figure 2 shows the optimized structure of **TS2$^-$**, which is 28.8 kJ/mol higher in energy than **2$^-$** and has only one imaginary frequency at 47i cm^{-1}. This vibrational mode is associated with the reaction coordinate that involves rotation of the non-coordinated py-NH moiety.
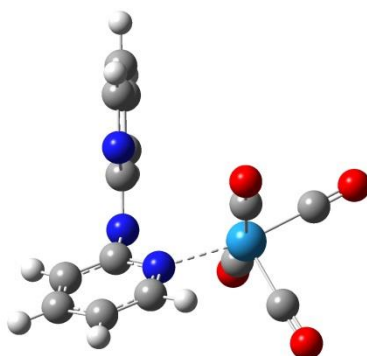
Fig. 2. Transition State $^{TS}2^-$ obtained from 2^- in which one py ring undergoes rotation.

Following this rotation by the intrinsic reaction coordinate method (IRC), as implemented in Gaussian 09, the subsequent fully geometry optimization resulted into a structure, 3^-, which is 10.1 kJ/mol lower in energy than 2^- (Figure 3).
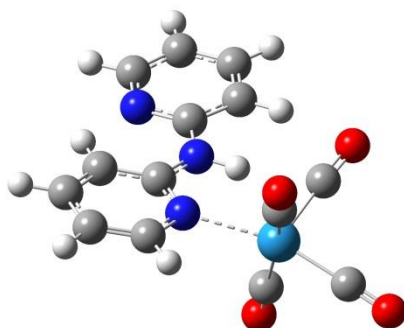

Fig. 3. Structure of 3^-.

The form 3^- displays an almost planar dpa ligand, with the NH group involved in an agostic W-H interaction (2.635 Å). Moreover, the hydrogen atom is close (2.252 Å) to an equatorial CO. As a matter of fact, in 3^- there is a vacant coordination position on W, free of steric hindrance. In MeCN solution and under inert atmosphere, this position is very probably occupied by a solvent molecule. This structure, however, does not account yet for the IR-SEC data, since the experimental ν_{CO} values are significantly higher than the computed ones (1916, 1809, 1800 and 1754 cm^{-1}), suggesting that 3^- still possess too high metal-centred electron density. A way to lower this character is by filling the vacant coordination site. This could be accomplished by the NH moiety either by a simple long-range interaction or by a net hydrogen transfer from NH to W (thus giving an hydride specie). By considering that COs are very likely fluxional, the W(CO)$_4$ fragment could be rearranged as in 4^- (Figure 4, right). The energy barrier that accounts for the transformation of 3^- into 4^- via $^{TS}3^-$ (Figure 4 left) is 24.9 kJ/mol.
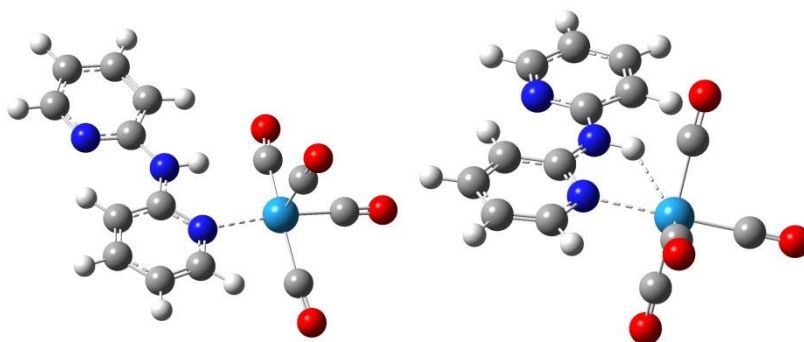

Fig. 4. Structure of $^{TS}3^-$ (left) and 4^- (right).

4⁻ is 5.3 kJ/mol lower in energy than **2⁻** and 4.8 kJ/mol higher than **3⁻**. The agostic W-H interaction in **4⁻** displays almost the same W-H distance (2.631 Å) of **3⁻**, but the vacant coordination site of W is now in front of the H atom. This structure has still a high metal-centred electron density (see Table 1), and cannot account for the IR-SEC data. Based on our precedent experience [11], we thought that H transfer with formation of the hydride could account both for the reduced electron density on the metal, as well as the vanishing of the NH stretching mode in IR-SEC. Indeed, the hydride **5⁻** has been found (Figure 5 right), and its ν_{CO} reflects the reduced electron density on W (see Table 1), albeit a little too much. However, **5⁻** is 33.9 kJ/mol higher in energy than **4⁻**, and the energy barrier (**ᵀˢ4⁻**, Figure 5 left) is 82.5 kJ/mol (only one imaginary frequency at 827i cm⁻¹; associated with the reaction coordinate involving the motion of H atom toward breaking the N-H bond and forming the W-H bond). Although we cannot exclude this side reaction pathway, the higher energy barrier seems to make less probable the hydride formation.
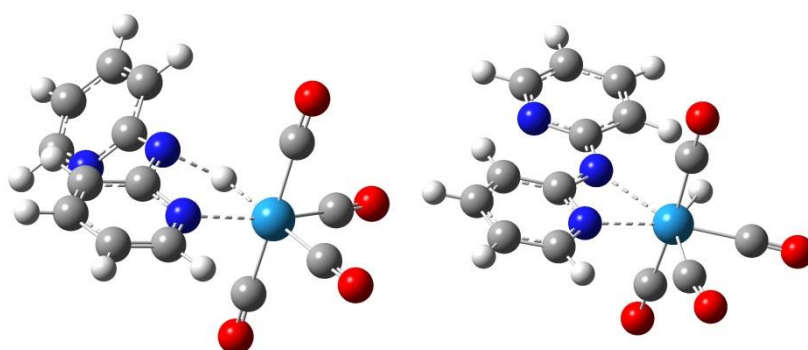

Fig. 5. Transition State **ᵀˢ4⁻** (left) for the process that leads to the formation of the hydride **5⁻** (right).

The agostic W-H interactions in **3⁻** and **4⁻** slightly weaken the N–H bond (Table 1). It is also worth to mention that during the electrochemical reduction of **2** small amounts of H₂ were detected [13]. Therefore, we think that the release of H₂ from **3⁻** or **4⁻** occurs more easily, being the simplest hypothesis to account for both the decrease of electron density on the metal and the disappearing of $\nu_{N–H}$. Removing H either from **3⁻** or **4⁻** resulted in the same structure **6⁻** (Figure 6a).
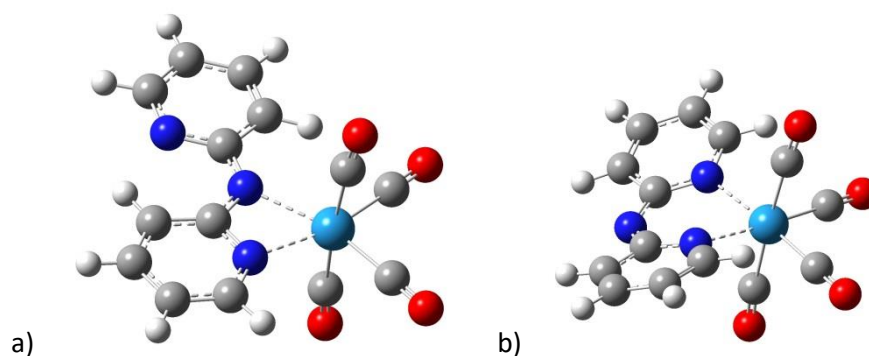

Fig. 6. The optimized structure of **6⁻** (a) and **7⁻** (b) after removing H.

The $\nu_{C–O}$ are in good agreement with the experimental data (Table 1), and both the equatorial (1.972 Å) and axial (2.043 Å) W-CO bonds are still short. The dehydrogenation could proceed as reaction among **2⁻**, **3⁻** and **4⁻** (in any combination), producing H₂ and **6⁻** or **7⁻** (obtained by removing H from **2⁻**, see Figure 6b). All the possible hydrogen evolution reactions are strongly thermodynamically favoured (computed ΔG ranges from –228.9 to –250.5 kJ per mol of H₂ produced). **3⁻** and **4⁻** leads to **6⁻**, while **2⁻** generates **7⁻** after H removal. The hydride **5⁻**, if formed, could also be involved in the hydrogen production.

The py rings of dpa that coordinate **7⁻** are bent by 28.6° with respect to the equatorial plane, and now the two py rings are tilted by 16.5° one respect the other. The two equatorial W-CO bonds are still shorter (1.973 Å)

in comparison with the two axial COs (~2.044 Å), suggesting that metal-carbonyl bonds are stable also for the anion 7^-. The computed DFT frequencies are in good agreement with the experimental ones (Table 1). The direct transformation of 7^- into 6^- is unlikely, because the energy barrier of the transition state is 98.2 kJ/mol (one imaginary frequency at 169i cm^{-1}).

The catalytic mechanism under CO_2 atmosphere is more difficult to explore, because faster kinetics of the homogeneous chemical reactions. However, it is known that carbonyl complexes very often releases CO after electrochemical reduction, because it is a way to reduce the electron density localized on the metal centre [27]. This is indeed what occurs after 2e reduction to **1** and similar $W(CO)_4(bpy)$ complexes. Although we demonstrated that 2^- undergoes 1e irreversible reduction (rearranging to 3^-) and does not release CO in long time, the reduction occurs at very negative potentials (very close to the second reduction of **1**), so that it seems reasonable to suppose that an equilibrium involving CO dissociation exists. Under inert gas the CO dissociation is not thermodynamically favoured, but under CO_2 the following equilibriums could be written involving either 3^- or its corresponding dehydrogenated counterpart 6^-:

$$3^- + CO_2 + e^- \leftrightarrow 8^{2-} + CO$$

$$6^- + CO_2 + e^- \leftrightarrow 9^{2-} + CO$$
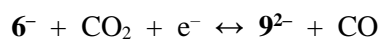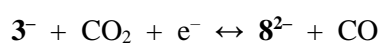
As a matter of fact, we optimized the two stable intermediates 8^{2-} and 9^{2-} (Figure 7a) in which the coordinated CO_2 is strongly bent (124° and 135° for 8^{2-} and 9^{2-}, respectively).
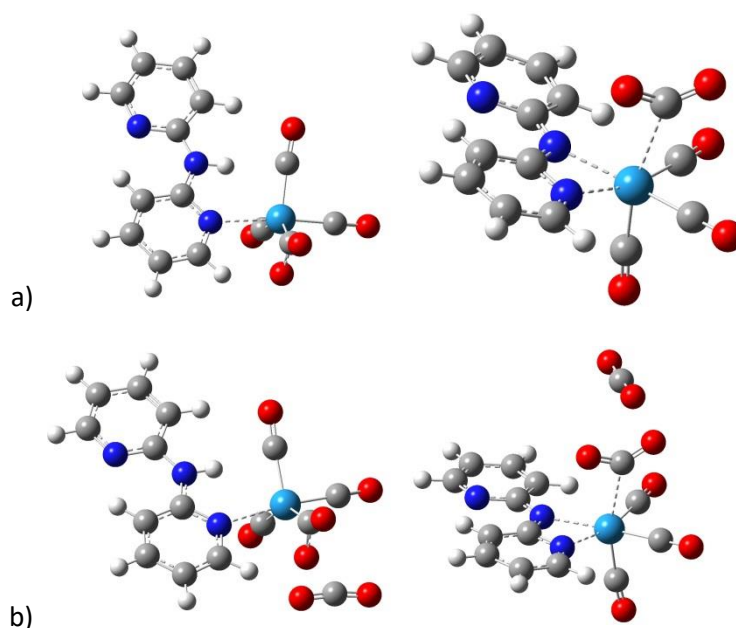

Fig. 7. a) Structure of 8^{2-} (left) and 9^{2-} (right), and b) optimized structures of $8^{2-}\cdot CO_2$ (left) and $9^{2-}\cdot CO_2$ (right) showing the interaction with another CO_2 molecule.

Both these species are able to give a significant interaction with another CO_2 molecules (Figure 7b), in which the non-coordinated CO_2 are bent of 170° and 175° in $8^{2-}\cdot CO_2$ and $9^{2-}\cdot CO_2$, respectively. The energy barriers of the transition states that lead to the formation of carbonate ions (Figure 8) are 27.5 kJ/mol for $8^{2-}\cdot CO_2$ (one imaginary frequency at 121i cm^{-1}), and 20.4 kJ/mol for $9^{2-}\cdot CO_2$ (one imaginary frequency at 148i cm^{-1}). The geometry of $^{TS}8^{2-}\cdot CO_2$ is biased towards the already formed CO_3^{2-}, and the final product containing the CO_3^{2-} ion is 71.4 kJ/mol more stable than $8^{2-}\cdot CO_2$. For $^{TS}9^{2-}\cdot CO_2$ the product containing carbonate ion is 17.7 kJ/mol less stable than $9^{2-}\cdot CO_2$. The release of CO_3^{2-} for both $8^{2-}\cdot CO_2$ and $9^{2-}\cdot CO_2$ affords **3** and **6**, respectively, which are promptly reduced to the corresponding anions at the working potential, shifting the equilibrium towards the production of carbonate ion.
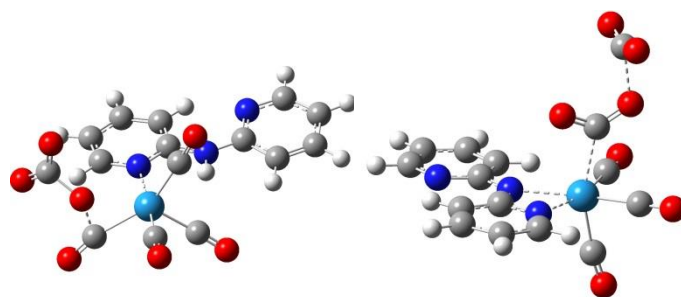
Fig. 8. Transition states $^{TS}8^{2-}\cdot CO_2$ (left) and $^{TS}9^{2-}\cdot CO_2$, (right) that leads to the formation of CO_3^{2-} from $8^{2-}\cdot CO_2$ and $9^{2-}\cdot CO_2$, respectively.

Conclusions

While in the case of **1** the 1e reduction affords a stable radical anion (only after a further 1e reduction it undergoes CO loss), the irreversible 1e reduction of compound **2** has been explained in terms of chemical rearrangement due to rotation of a pyridine ring of the dipyridylamine ligand. No CO loss is predicted also by DFT. For both complexes there is a reasonable agreement between experimental IR-SEC and computed DFT IR frequencies. At long time of the IR-SEC experiments deprotonation accounts for the observed IR spectra in **2**. The energy profile of the chemical rearrangement induced by the reduction is summarized in Figure 9a. A catalytic mechanism of CO_2 reduction in MeCN solutions of **2** has been proposed, involving the coordination of a CO_2 that is expected to interact with another CO_2, leading to the formation of carbonate ion. Two pathways were explored, highlighting that the deprotonation of NH in the reduced **2** makes less favourable the catalytic cycle, due to enhanced stability of 6^-. Thus, this study suggests that the deprotonation, and subsequent decomposition reactions, could be among the reasons of catalytic deactivation. Finally, a reasonable mechanism that leads to the formation of CO and carbonate ion has been proposed. The overall energy profile is summarized in Figure 9b.[28]
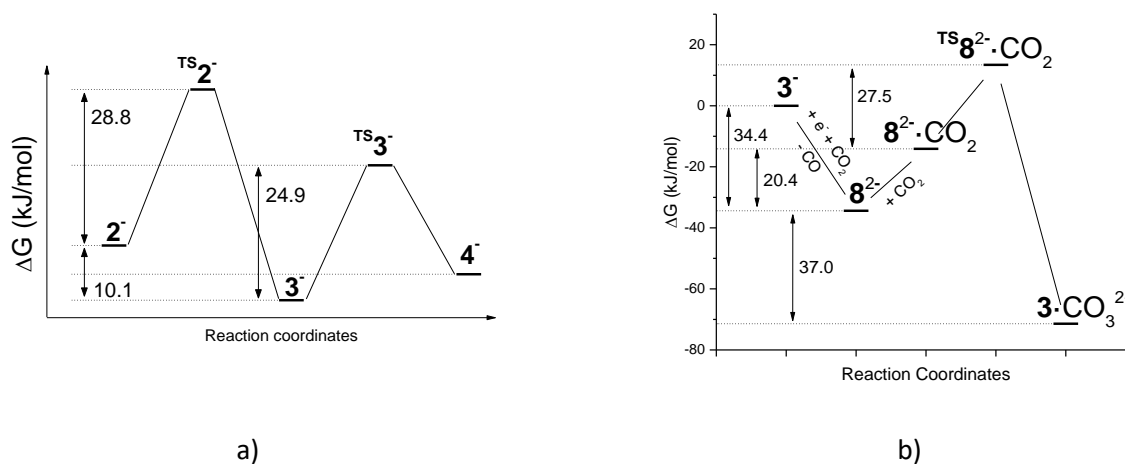

a)

b)

Fig. 9. Energy profile for the chemically irreversible reduction of **2** (a), and the overall energetics leading to the formation of CO and CO_3^{2-} (b).

5. Acknowledgements

Supplementary Data

Optimized geometries of all complexes.

References

[1] M. Aresta, A. Dibenedetto, A. Angelini, Chem. Rev., 114 (2014) 1709-1742.

[2] N. Armaroli, V. Balzani, Chem. Eur. J., 22 (2016) 32-57.

[3] J. Ronge, T. Bosserez, D. Martel, C. Nervi, L. Boarino, F. Taulelle, G. Decher, S. Bordiga, J.A. Martens, Chem. Soc. Rev., 43 (2014) 7963-7981.

[4] S. Berardi, S. Drouet, L. Francas, C. Gimbert-Surinach, M. Guttentag, C. Richmond, T. Stoll, A. Llobet, Chem. Soc. Rev., 43 (2014) 7501-7519.

[5] N. Armaroli, V. Balzani, Angew. Chem. Int. Ed. Engl., 46 (2007) 52-66.

[6] J. Bonin, A. Maurin, M. Robert, Coord. Chem. Rev., 334 (2017) 184-198.

[7] C. Costentin, M. Robert, J.-M. Saveant, Chem. Soc. Rev., 42 (2013) 2423-2436.

[8] N. Elgrishi, M.B. Chambers, X. Wang, M. Fontecave, Chem. Soc. Rev., 46 (2017) 761-796.

[9] F. Franco, C. Cometto, C. Garino, C. Minero, F. Sordello, C. Nervi, R. Gobetto, Eur. J. Inorg. Chem., (2015) 296-304.

[10] F. Franco, C. Cometto, F. Ferrero Vallana, F. Sordello, E. Priola, C. Minero, C. Nervi, R. Gobetto, Chem. Commun., 50 (2014) 14670-14673.

[11] F. Franco, C. Cometto, L. Nencini, C. Barolo, F. Sordello, C. Minero, J. Fiedler, M. Robert, R. Gobetto, C. Nervi, Chem. Eur. J., 23 (2017) 4782-4793.

[12] F. Franco, C. Sun, C. Cometto, R. Gobetto, C. Nervi, in: Synthesis and Electrochemical Studies of Rhenium(I) and Molybdenum(0) Complexes as Electrocatalysts for Reduction of Carbon Dioxide, 46th Heyrovsky Discussion, Heyrovsky Institute, Trest (Czech Republic), 2013, pp. 63-63; ISBN: 978–80–87351–24–6.

[13] F. Franco, C. Cometto, C. Minero, L. Nencini, J. Fiedler, R. Gobetto, C. Nervi, ChemElectroChem, 2 (2015) 1372-1379.

[14] K.A. Grice, C. Saucedo, Inorg. Chem., 55 (2016) 6240-6246.

[15] M.L. Clark, K.A. Grice, C.E. Moore, A.L. Rheingold, C.P. Kubiak, Chem. Sci., 5 (2014) 1894-1900.

[16] J. Tory, B. Setterfield-Price, R.A.W. Dryfe, F. Hartl, ChemElectroChem, 2 (2015) 213-217.

[17] A. Dubey, L. Nencini, R.R. Fayzullin, C. Nervi, J.R. Khusnutdinova, ACS Catalysis, 7 (2017) 3864-3868.

[18] A. Bucci, G. Menendez Rodriguez, G. Bellachioma, C. Zuccaccia, A. Poater, L. Cavallo, A. Macchioni, ACS Catalysis, 6 (2016) 4559-4563.

[19] M.J. Frisch, G.W. Trucks, H.B. Schlegel, G.E. Scuseria, M.A. Robb, J.R. Cheeseman, G. Scalmani, V. Barone, B. Mennucci, G.A. Petersson, H. Nakatsuji, M. Caricato, X. Li, H.P. Hratchian, A.F. Izmaylov, J. Bloino, G. Zheng, J.L. Sonnenberg, M. Hada, M. Ehara, K. Toyota, R. Fukuda, J. Hasegawa, M. Ishida, T. Nakajima, Y. Honda, O. Kitao, H. Nakai, T. Vreven, J.A.J. Montgomery, J.R. Peralta, F. Ogliaro, M. Bearpark, J.J. Heyd, E. Brothers, K.N. Kudin, V.N. Staroverov, R. Kobayashi, J. Normand, K. Raghavachari, A. Rendell, J.C. Burant, S.S. Iyengar, J. Tomasi, M. Cossi, N. Rega, J. Millam, M. Klene, J.E. Knox, J.B. Cross, V. Bakken, C. Adamo, J. Jaramillo, R. Gomperts, R.E. Stratmann, O. Yazyev, A.J. Austin, R. Cammi, C. Pomelli, J. Ochterski, R.L. Martin, K. Morokuma, V.G. Zakrzewski, G.A. Voth, P. Salvador, J.J. Dannenberg, S. Dapprich, A.D. Daniels, O. Farkas, J.B. Foresman, J.V. Ortiz, J. Cioslowski, D.J. Fox, in, Gaussian, Inc., Wallingford CT, 2009.

[20] S. Miertuš, E. Scrocco, J. Tomasi, Chem. Phys., 55 (1981) 117-129.

[21] P.J. Hay, W.R. Wadt, J. Chem. Phys., 82 (1985) 270-283.

[22] J.P. Merrick, D. Moran, L. Radom, J. Phys. Chem. A, 111 (2007) 11683-11700.

[23] R.A. Howie, G. Izquierdo, G.P. McQuillan, Inorg. Chim. Acta, 72 (1983) 165-172.

[24] C.M. Bolinger, N. Story, B.P. Sullivan, T.J. Meyer, Inorg. Chem., 27 (1988) 4582-4587.

[25] S. Slater, J.H. Wagenknecht, J. Am. Chem. Soc., 106 (1984) 5367-5368.

[26] B.K. Teo, A.P. Ginsberg, J.C. Calabrese, J. Am. Chem. Soc., 98 (1976) 3027-3028.

[27] P. Zanello, C. Nervi, F. Fabrizi De Biani, Inorganic Electrochemistry. Theory, Practice and Application, 2nd ed., RSC, Cambridge, 2011.

[28] The Gibbs free energy of the reduction of $\mathbf{3^-}$ giving $\mathbf{8^{2-}}$ has been estimated computing the energy of $\mathbf{3^{2-}}$, since direct comparison between the energies of species with different numer of electrons is usually not possible.